Available online at www.sciencedirect.com
SCIENCE DIRECT
Biochimica et Biophysica Acta 1758 (2006) 772–780
BIOCHIMICA ET BIOPHYSICA ACTA
BBA
http://www.elsevier.com/locate/bba

The structural properties of the transmembrane segment of the integral membrane protein phospholamban utilizing ^{13}C CPMAS, ^{2}H, and REDOR solid-state NMR spectroscopy

Ethan S. Karp, Elvis K. Tiburu, Shadi Abu-Baker, Gary A. Lorigan *

Department of Chemistry and Biochemistry, Miami University, Oxford, OH 45056, USA

Received 23 January 2006; received in revised form 22 March 2006; accepted 4 April 2006
Available online 19 May 2006

Abstract

Solid-state NMR spectroscopic techniques were used to investigate the secondary structure of the transmembrane peptide phospholamban (TM-PLB), a sarcoplasmic Ca^{2+} regulator. ^{13}C cross-polarization magic angle spinning spectra of ^{13}C carbonyl-labeled Leu39 of TM-PLB exhibited two peaks in a pure 1-palmitoyl-2-oleoyl-phosphocholine (POPC) bilayer, each due to a different structural conformation of phospholamban as characterized by the corresponding ^{13}C chemical shift. The addition of a negatively charged phospholipid (1-palmitoyl-2-oleoylphosphatidylglycerol (POPG)) to the POPC bilayer stabilized TM-PLB to an α-helical conformation as monitored by an enhancement of the α-helical carbonyl ^{13}C resonance in the corresponding NMR spectrum. ^{13}C–^{15}N REDOR solid-state NMR spectroscopic experiments revealed the distance between the ^{13}C carbonyl carbon of Leu39 and the ^{15}N amide nitrogen of Leu42 to be 4.2±0.2Å indicating an α-helical conformation of TM-PLB with a slight deviation from an ideal 3.6 amino acid per turn helix. Finally, the quadrupolar splittings of three ^{2}H labeled leucines (Leu28, Leu39, and Leu51) incorporated in mechanically aligned DOPE/DOPC bilayers yielded an 11°±5° tilt of TM-PLB with respect to the bilayer normal. In addition to elucidating valuable TM-PLB secondary structure information, the solid-state NMR spectroscopic data indicates that the type of phospholipids and the water content play a crucial role in the secondary structure and folding of TM-PLB in a phospholipid bilayer.

Keywords: Solid-state nuclear magnetic resonance spectroscopy; Phospholamban; REDOR; Membrane protein; Transmembrane domain; ^{13}C CPMAS; Peptide tilt

1. Introduction

Nuclear Magnetic Resonance (NMR) is a rapidly growing technique to study large proteins, especially those that are hydrophobic and for which crystallized forms unavailable [1–6]. The protein of interest in the current study is the transmembrane segment of a 52 amino acid integral membrane protein, phospholamban (TM-PLB). PLB is involved in the regulation of calcium across sarcoplasmic reticulum (SR) membranes in cardiac muscle cells [7]. After the release of Ca^{2+} during cardiac muscle contraction, the calcium ATPase known as SERCA reuptakes the calcium across the SR through a mechanism hypothesized to involve a high Ca^{2+} affinity to low Ca^{2+} affinity conformation [8]. Non-phosphorylated PLB inhibits this SERCA conformation change through a mechanism that is not well understood [9, 10]. Phosphorylation of PLB at Ser16 and Thr17 lifts the inhibition of the SERCA conformation change. It is hypothesized that a conformation change of PLB when phosphorylated may be the mechanism of PLB inhibition [11]. To understand the conformation change of PLB, the structure of wild-type PLB in its natural lipid must be explored first. Often a cysteine to alanine mutant of TM-PLB is studied but the current study explores the naturally occurring wild-type TM-PLB. Elucidating the mechanism of PLB SERCA inhibition is very important as it has recently been discovered that simple point mutations in PLB result in dilated cardiomyopathy and congestive heart failure at young ages [8,12].

Phospholamban consists of three structural domains: residues 1–20 which comprise the hydrophilic cytoplasmic domain, residues 21–30 that represent a short hinge or β-sheet segment, and residues 31–52 that encompass the hydrophobic α-helical membrane-spanning region [13–15]. There is still disagreement on the structure of PLB embedded inside phospholipid membranes

* Corresponding author. Tel.: +1 513 529 3338; fax: +1 513 529 5715.
E-mail address: lorigag@muohio.edu (G.A. Lorigan).

0005-2736/$ - see front matter © 2006 Elsevier B.V. All rights reserved.
doi:10.1016/j.bbamem.2006.04.016

even though studies have suggested that PLB readily associates in lipid bilayers to form a homopentamer [11,16,17]. Chou and coworkers have recently conducted solution-state NMR experiments on the proposed pentameric form of PLB reconstituted in DPC micelles. These results suggest that the transmembrane segment of PLB is a tilted α-helical in the bilayer [18]. The specific alignment of the five helices have been supported by Li's mutagenic studies, which indicate a specific orientation of PLB, with Leu42 and Leu39 near the lipid side of the pentamer [7]. Currently, there are three structural models that have been proposed based upon spectroscopic studies and molecular modeling techniques for pentameric PLB [19,20]. In one model, PLB is composed of two α-helices connected by an unstructured/β-sheet region with the cytosolic domain tilted approximately 50°–70° with respect to the bilayer normal [18,19]. Another structural model suggests a continuous α-helix with a tilt angle of about 28° for PLB with respect to the bilayer normal [20]. Finally, a recent solution NMR paper indicates that pentameric WT-PLB forms a channel architecture with an unusual bellflower-like assembly for the cytoplasmic segment [18]. Each of these structural models has implications on the tilt angle of the TM-PLB with respect to the bilayer.

As mentioned above, many experiments have analyzed the monomeric form of PLB by mutating three PLB transmembrane Cys with Ala residues, which inhibit the formation of pentameric PLB [9,21,22]. ^{15}N-labeled solid-state NMR spectroscopic studies on the AFA-PLB have indicated that the monomeric form of PLB has one component that is nearly transmembrane (hydrophobic segment, residues 31–52) and another segment (cytosolic region) that lies on the surface of the membrane [13]. The monomeric transmembrane helix makes an approximate 10° angle with respect to the bilayer normal [13].

Previously, the solid-state NMR spectroscopic technique of rotational-echo double-resonance (REDOR) on the monomeric, mutated form of phospholamban has been used to determine the distance between residues ^{15}N-Leu37 and 1 Leu39 of transmembrane PLB incorporated into dimyristoylphosphatidylcholine (DMPC) membranes [23]. The experiment yielded a distance of 3.2±0.2 Å. This value is very close to the distance of 3.26 Å expected for an α-helical structure. In addition to the REDOR results supporting the α-helical structure for monomeric PLB, rotational resonance NMR data has been used to measure the ^{13}C homonuclear dipolar couplings between Leu42 and Cys46 which is consistent with an α-helical conformation of monomeric PLB [11,23,24]. In the present study, we will probe not the monomeric form, but the pentameric form of naturally occurring TM-PLB in longer chain POPC and DOPC phospholipid bilayers.

Three powerful solid-state NMR techniques that are often used to probe the structural properties of integral membrane proteins are ^{13}C-CPMAS, ^{2}H NMR, and REDOR spectroscopy [25–29]. ^{13}C cross-polarization magic angle spinning (CPMAS) is a solid-state NMR spectroscopic technique that reveals isotropic chemical shift spectra of solid powder samples. For peptides and proteins, the isotropic chemical shift of the ^{13}C carbonyl carbon of amino acids depends upon the backbone torsion angles and hydrogen-bonding pattern, resulting in a strong correlation with the secondary structure [30–35]. In solution NMR spectroscopy, certain solvents are known to induce α-helical secondary structural folding patterns. Similarly in lipid bilayers, factors such as lipid:protein ratio, lipid charge, lipid composition, and hydration level can affect the protein folding pattern. Thus, in this study the effects of lipid charge and hydration on the secondary structure of TM-PLB with ^{13}C CPMAS was explored. ^{2}H NMR spectroscopy of specifically labeled amino acid sidechains of proteins can be used to determine the tilt angle of a peptide in a membrane and REDOR can be used to determine inter-amino acid distances in proteins. The above three techniques have been combined to study the folding and secondary structure of PLB in lipid bilayers.

2. Materials and methods

2.1. Materials

Fmoc-amino acids and other chemicals for peptide synthesis were purchased from Applied Biosystems Inc. (Forster City, CA). Fmoc-leucine-^{15}N derivatives and ^{2}H-depleted water were purchased from Isotec (Miamisburg, OH). 1,2-dioleoyl-phosphocholine (DOPC), 1,2-dioleoyl-phosphoethanolamine (DOPE), 1-palmitoyl-2-oleoyl-phosphocholine (POPC), and 1-palmitoyl-2-oleoylphosphatidylglycerol (POPG) were purchased from Avanti Polar Lipids Inc. (Alabaster, AL). The phospholipids were shipped already dissolved in chloroform at a concentration of 20 mg/mL and stored at −20 °C. Chloroform, hexafluoro-2-propanol (HFIP), formic acid and 2,2,2-trifluoroethanol (TFE) were purchased from Sigma-Aldrich Chemical Co. (St. Louis, MO). HPLC-grade acetonitrile and isopropanol were obtained from Pharmco (Brockfield, CT) and were filtered through a 0.22-μm nylon membrane before use. Water was purified using a nanopure reverse osmosis system (Millipore, Bedford, MA). N-2-hydroxyethyl piperizine-N-2-ethane sulfonic acid (HEPES), triflouro acetic acid (TFA), and EDTA were also obtained from Sigma-Aldrich (St. Louis, MO).

2.2. Peptide synthesis

^{13}C and ^{15}N site-specific isotopically labeled polypeptides corresponding to TM-PLB Ala24-Leu52 ARQN(^{2}H-L)QNLFINFC(^{2}H-L)I(^{13}C-L)IC(^{15}N-L)LLICIIVM(^{2}H-L)L with the specific labels indicated were synthesized on an Applied Biosystems Inc. (ABI) 433A solid-phase peptide synthesizer controlled by a G3 Macintosh computer with SynthAssist™ 2.0 software as described previously [36]. Each deuterium labeled peptide was created individually and one dually labeled ^{13}C, ^{15}N sample was made for REDOR thus making four PLB peptides in all.

2.3. Peptide purification

The synthesized peptides were removed from the synthesizer and cleaved from the resin. The lyophilized peptides were dissolved in HFIP/FA (4:1, at a concentration of 5 mg/mL) and centrifuged to eliminate insoluble particulates. The crude peptides were purified on an Amersham Pharmacia Biotech AKTA® Explorer 10S HPLC controlled by Unicorn™ version 3 system software. A polymer-supported column (259 VHP82215, 5 μm, 300 Å pore size, 2.2×15 cm) from Grace-Vydacc was used to purify PLB. The column was equilibrated with 95% solvent A:5% solvent B. Solvent A consisted of H_2O+0.1% TFA and solvent B was 38% MeCN+57% IPA+5% H_2O. A 1 mL aliquot of the (5 mg/mL) peptide sample was injected into the column and the gradient was ramped from 5% to 100% of Solvent B at a flow rate of 10 mL/min. Peptide elution was achieved with a linear gradient to a final solvent composition of 93% solvent B. The purified peptide fraction was lyophilized and analyzed by MALDI-TOF mass spectroscopy using a matrix of 2,5-dihydroxybenzoic acid. The overall yield of TM-PLB was about 37% [36].

2.4. Sample Preparation for ^{13}C CPMAS and REDOR experiments

For the ^{13}C CPMAS and REDOR experiments, 4 mol% protein with respect to lipid was used. The lipid was either in a 3:1 ratio of POPC to POPG or pure

POPC. The PLB was first dissolved in 100μL of TFE and 100 μL of chloroform, and vortexed. To this mixture the lipids were added slowly, then transferred to a small test tube. The resultant solution was then sonicated in a Fischer sonicator with the heater turned off while covered for 15 min. Under a light stream of N_2 gas, the test tube was dried until all the chloroform was removed. The test tube was then placed in a vacuum dessicator overnight.

The resultant paste was packed tightly into a 4-mm diameter zirconium oxide MAS NMR rotor purchased from Bruker. The inhomogeneity of the B_0 field was minimized by filling the rotor to 50% of the total volume and by centering the sample [37]. Using a small syringe, five or six holes were punched into the sample, and the rotor was placed in a 100% humidity chamber for 20 h to complete the hydration process. Whenever the rotor was not in use, it was stored at −20 °C in a freezer.

2.5. Sample preparation for mechanically aligned ^2H experiments

The mechanically aligned samples were prepared by dissolving PLB in a minimal amount of TFE and the solution was mixed with DOPC/DOPE (4:1 mole ratio) dissolved in chloroform in a pear-shaped flask. Nitrogen gas was passed over the resulting mixture to reduce the volume of the chloroform to a third of the original volume. The sample was spread onto 25 glass plates of dimensions 8.5 mm × 14 mm and the glass plates were allowed to dry in a dessicator overnight. The peptide to lipid mole ratio was 1:100. Deuterium-depleted water was added onto the lipid–peptide mixture and the glass plates were stacked on top of each other. The stacked glass plates were then placed in a humidity chamber of ammonium monophosphate at a relative humidity of about 93% at 42 °C for 24 h.

2.6. Solid-state NMR spectroscopy

All NMR experiments were conducted on a 11.7 T Bruker AVANCE 500 MHz wide bore solid-state NMR spectrometer. The ^1H–^{13}C CPMAS NMR experiments were performed with a Bruker triple-resonance CPMAS probe at ^1H, ^{13}C and ^{15}N resonance frequencies of 500.13, 125.78 and 50.68 MHz, respectively. The ^1H 90° pulse length was 4.5 μs. Cross polarization was performed with a contact time of 1.5 ms, ^1H decoupling with a field of 60 kHz, recycle delay of 3 s, and 16,000 scans were signal averaged [38]. The spinning speed was controlled at 6000 ± 1 Hz at a temperature of − 50 °C. Lorentzian line broadening of 100 Hz was applied before Fourier transformation. All ^{13}C chemical shifts were referenced relative to tetramethylsilane (TMS) at 0 ppm. For the mechanically aligned ^2H samples, a double resonance flat coil solid-state NMR probe of dimension 8.5 mm × 14 mm was used operating at 25 °C and 40 °C. The quadrupolar echo pulse sequence was used with quadrature detection capabilities and complete phase cycling of the pulse pairs [39]. A 3.0-μs 90° pulse, a sweep width of 100 kHz, a recycle delay time of 400 ms, and a 30-μs interpulse delay were used to accumulate 150,000 transients. Prior to Fourier transformation, an exponential multiplication of 200 Hz line broadening was performed on the spectra. Nearly identical ^2H NMR spectra were obtained at both 25 °C and 40 °C for the mechanically aligned TM-PLB samples.

The REDOR data were collected using a series of ^{15}N π pulses with two pulses per rotor cycle [40]. Phase cycling (XY8) was used to compensate for errors in the flip angle, resonance offset effect and variation in the B_1 field [40]. A single ^{13}C π pulse was used to refocus the chemical shift interaction. The spinning speed was controlled at 6000 and 8000 ± 1 Hz at a temperature of −50 °C. ^1H, ^{13}C and ^{15}N 90° pulse lengths were 4.5 μs, 6.2 μs and 7 μs, respectively. The ^1H–^{13}C CP contact time was 1.5 ms, and a ^1H TPPM decoupling of 60 kHz was applied during both dephasing and detection periods [40]. The number of transients ranged from 16,000 to 32,000 to achieve reasonable signal to noise ratios.

2.7. ^2H Tilt Angle Analysis

The helical tilt angles for ^2H were calculated using equations previously derived in the literature [41–44]. The observed quadrupolar splitting ($\Delta\nu_q$) for a deuterated amino acid side chain in a peptide incorporated into aligned spectra can be expressed as [41–44]:

$$\Delta\nu_q = (3/4)K(3\cos^2\varepsilon_{\|}(\cos\tau - \sin\tau\cos\delta\tan\varepsilon_{\|})^2 - 1) \quad (1)$$

where $e_{\|}$ is the angle between the peptide helical axis and the side chain bond vector, τ is the tilt angle defined as the angle between the peptide helix axis and the bilayer normal (assumed to be along the magnetic field direction), and K is the quadrupolar coupling constant [41]. δ is the rotation angle that depends on the three angles shown below

$$\delta = \rho + \varepsilon_{\perp} + \tau \quad (2)$$

where ρ is the rotation of the helix when compared to a standard orientation, $e_{\perp}$ is the angle of the bond vector with respect to a vector of the side chain to the peptide axis, and φ is the angle between a reference residue and a labeled residue given by (n-1)*100 where n is the number of residues from the reference residue. K is given by

$$K = (e^2qQ/h)S \quad (3)$$

where e^2qQ is the quadrupole interaction, h is Planck's constant, and S is the order parameter. The tilt angle of the protein in DOPC bilayers was calculated using a program written in C++. The parameter ρ was varied from 0 to 360° in increments of 0.1° and τ was varied from 0 to 50° in increments of 0.1°. Values for $e_{\|}$ and $e_{\perp}$ of each leucine residue were gathered assuming that the C − D bond vectors were averaged about the Cγ − Cδ bond. Leu28 was chosen as the arbitrary reference amino acid with ρ=0°. The root mean squared deviation (RMSD) was used to rank the possible values of ρ and τ. From modeling using Insight II software and using the Mol–Mol molecular modeling software and phospholamban model from the protein data bank (model 1FJK) [45], $e_{\|}$=70° and $e_{\perp}$=32° for the leucine residues used in this study. For fast methyl group rotation, the quadrupolar coupling constant was reduced by two third thirds [46,47]. Thus, a quadrupolar coupling constant of 19 kHz was used for the tilt angle calculations.

2.8. REDOR analysis and theory

REDOR NMR measures the dipolar interaction between two different nuclei, which is inversely proportional to the cube of the internuclear distance [48–54]. The net result of this pulse sequence is a decrease in intensity of the observed nuclei chemical shift peak. The magnitude of this decrease is given by:

$$\Delta S/S_0 = 1/2\pi \int_0^{\pi}\int_0^{\pi} \cos(\phi)\sin(\beta)d\beta d\alpha \quad (4)$$

where S_r is the reduced signal and S_0 is the signal created by the REDOR pulse sequence applied to the I nucleus without any pulses on the S nuclei. The distance between the I and S nuclei can be found after curve fitting the experimental data to equation 4 by using [54]

$$r = (\varepsilon_0 h\gamma_C\gamma_N/(16\pi^2 D)) \quad (5)$$

where ε_0 is the permeativity of free space, γ_C and γ_N are the gyromagnetic ratios of ^{13}C and ^{15}N, respectively. In the present experiment, the I nucleus is ^{13}C and the S nucleus is ^{15}N [51]. Maximum distance measurements using these nuclei are on the order of 5 Å [50]. Microsoft Excel was used to simulate the $\Delta S/S_0$ versus $N_c T_r D$ (dephasing time) curves where $\Delta S = |S_r - S_0|$, N_c is the number of rotor cycles before data acquisition, T_r is the rotor period, and D is the dipolar coupling constant.

3. Results

3.1. ^{13}C CP-MAS solid-state NMR spectroscopy on TM-PLB

^{13}C CPMAS solid-state NMR spectroscopy was used to investigate the effect of hydration and choice of phospholipids on the secondary structure and folding pattern of TM-PLB in phospholipid bilayers. Previous ^{31}P and ^2H solid-state NMR studies in our lab have indicated that TM-PLB incorporates into POPC to form multi-lamellar vesicles (MLVs) in the Lα phase [55]. Fig. 1A shows the carbonyl carbon region of the ^{13}C

CPMAS NMR spectrum of $^{13}C{=}O$ labeled Leu39 TM-PLB incorporated into pure POPC phospholipid bilayers upon hydration. The ^{13}C NMR spectra were similar for samples at temperatures ranging from −25 °C to 25 °C except an increase in the signal to noise ratio was observed at −25 °C. There are clearly two well-resolved peaks, one at 172.9 ppm and one at 175.9 ppm. The peak at 172.9 ppm corresponds to a β-sheet or an unstructured component of the peptide, whereas the peak at 175.9 ppm corresponds to an α-helical structure [24]. While it cannot be clearly seen, the natural abundance lipid ^{13}C carbonyl carbon chemical shift falls in between these two peaks at about 174 ppm. This resonance is not as pronounced as the two intense peaks originating from the ^{13}C-labeled Leu39 residue.

A second $^{13}C{=}O$ labeled Leu39 TM-PLB peptide sample was prepared with a mixture of lipids instead of using pure POPC. Negatively charged POPG was used along with POPC in a ratio of 3:1 (POPC:POPG). Fig. 1B shows the ^{13}C CPMAS NMR spectrum of this new sample prepared in the absence of hydration. The spectrum reveals that there are still two intense peaks, but the downfield peak, attributed to contributions from the α-helical structural conformation of the peptide, is much more intense and pronounced. The same sample was hydrated for 20 h and the resultant ^{13}C CPMAS NMR spectrum (Fig. 1C) yielded a pronounced change. The peak that was originally located at 172.9 ppm disappeared and the *S*/*N* ratio of the downfield peak increased dramatically. Thus, in the presence of POPC and POPG phospholipid bilayers, Leu39 of TM-PLB is predominantly folded into an α-helical structure. The small shoulder to the right of the 175.9 ppm peak is due to natural abundance carbonyl carbon from the lipids.

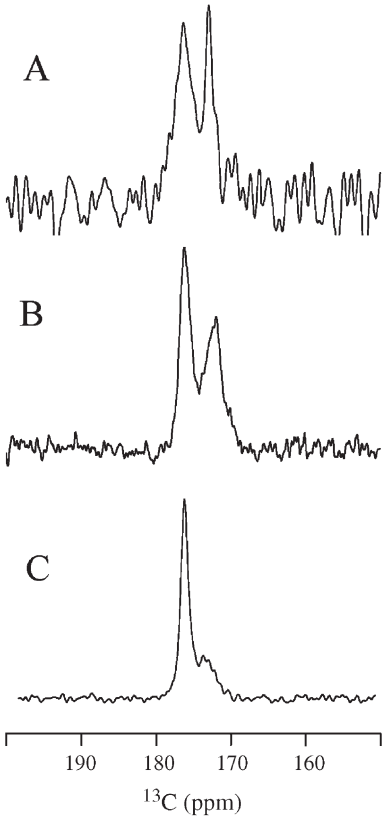

Fig. 1. ^{13}C-CPMAS solid-state NMR spectra of $^{13}C{=}O$ labeled Leu39 TM-PLB peptide prepared in different lipid/hydration environments at −25 °C. (A) TM-PLB in a hydrated POPC bilayer, (B) TM-PLB is a POPC/POPG 3:1 molar ratio without hydration, and (C) TM-PLB in a hydrated POPC/POPG 3:1 molar ratio. The intensity of the upfield peak increases in resolution and height when going from just POPC to the POPC/POPG mixture to the hydrated sample. CPMAS spinning speeds were varied with comparable results from 6000 to 8000 Hz and 8000 transients were taken for each ^{13}C CPMAS NMR spectrum.

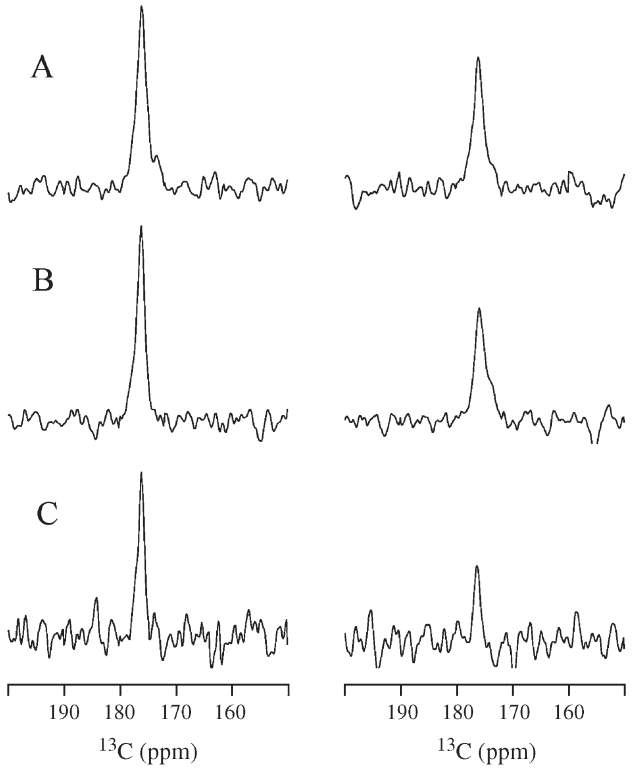

Fig. 2. Solid-State NMR ^{13}C–^{15}N REDOR data on a $^{13}C{=}O$ Leu39/^{15}N-Leu42 TM-PLB peptide reconstituted into hydrated POPC/POPG bilayers for heteronuclear distance measurements with dephasing times of (A) 12 ms, (B) 15 ms, and (C) 18 ms. The spectra on the left side correspond to the normal ^{13}C undephased S_0 reference solid-state NMR spectra. The spectra on the right side represent the dephased spectra in which the ^{15}N spins were excited.

3.2. ^{13}C–^{15}N REDOR spectroscopy of TM-PLB

In order to extend the secondary structural analysis of TM-PLB in phospholipid bilayers over a wider range of residues, REDOR spectroscopy was used. REDOR is a widely used solid-state NMR spectroscopic technique to probe heteronuclear dipolar distances [27,28,56–58]. In this study, the ^{13}C observed (^{15}N dephased) REDOR experiment measures the dipolar dephasing by comparing signal intensities in ^{13}C CPMAS NMR spectra collected with and without ^{15}N-dephasing π pulses. ^{13}C–^{15}N REDOR was used to determine the inter helix distance in the TM-PLB peptide. Fig. 2 shows representative ^{13}C observed REDOR spectra with (*S*) and without (S_0) the ^{15}N π pulses for the ^{13}C-Leu39/^{15}N-Leu42 TM-PLB peptide reconstituted into POPC/POPG bilayers. The resonance peak at 176 ppm corresponds to the single label $^{13}C{=}O$ on Leu39. The small shoulder observed at 174 ppm corresponds to the natural

abundance $^{13}C{=}O$ of the phospholipids. Efficient dephasing of the labeled ^{13}C-Leu39 resonance is observed in the REDOR spectrum above 12 ms. Four S_0 and S spectra were acquired at dephasing periods of 12, 15, 18 and 20 ms. Each pair of spectra were then analyzed to determine $\Delta S/S_0$ which is $(S_0-S)/S_0$. All of the dephased ^{13}C spectra decreased in intensity with the larger dephasing time. The $\Delta S/S_0$ values are plotted versus the dephasing time in Fig. 3 along with simulated REDOR curves corresponding to a ^{13}C–^{15}N distance between 4.0 Å and 4.4 Å. The REDOR experimental data points (diamonds) match well with the 4.2 Å REDOR simulated curve.

The near disappearance of the natural abundance lipid contribution to the ^{13}C signal in the REDOR experiment spectra (Fig. 2) is due to the relative motion of the lipids compared with the protein backbone. This is consistent with studies by Naito and coworkers and Cornell and coworkers that demonstrate the relatively low rate of motion of the protein melittin in DMPC bilayers compared to the motion of the lipids at low temperatures [59–61]. Even at −25 °C, motion of lipids such as DMPC have spin diffusion rates of the order 100 ns [62] while the protein backbone is frozen [63]. The contribution of the natural abundance lipid carbonyls to the spectra is no longer present because the signal has already diffused into the surrounding system before detection because of the large amount of time between pulsing the ^{13}C of the system and acquiring data.

3.3. ^{2}H NMR on mechanically aligned samples

The helical tilt of TM-PLB in mechanically aligned DOPC/DOPE phospholipid bilayers was next investigated with ^{2}H solid-state NMR spectroscopy. DOPC/DOPE phospholipid bilayers have been shown to be an excellent model phospholipid system for reconstituting PLB and should have very close bilayer widths to the POPC/POPG bilayers used in the ^{13}C and REDOR experiments [64]. The results of the ^{2}H NMR study of TM-PLB in DOPC/DOPE phospholipid bilayers on mechanically aligned glass plates are displayed in Fig. 4. The main components of these three spectra include a small splitting of 0.9 kHz for Leu28 (Fig. 4A), and larger splittings of 2.2 kHz and 2.5 kHz for Leu39 and Leu51, respectively (Fig. 4B and C). The isotropic peak in the center of the spectra is attributed to excess water in the system. The poor signal to noise is caused by the limited amount of peptide that will properly insert in mechanically alignable samples. The lineshapes of the aligned ^{2}H NMR spectra look dramatically different than those obtained from unoriented multi-lamellar vesicles (an example of an unoriented spectrum is shown in Fig. 4D and is taken from reference 16). Temperature did not have any major effect on the ^{2}H quadrupolar splittings shown in Fig. 4. The same splittings were obtained at both 25 °C and 40 °C for the mechanically aligned samples. A tilt angle of 11°±5° was found of TM-PLB with respect to the membrane normal [65]. Most of the error associated with the tilt angle is due to the inability to perfectly determine the S values for each labeled site and was estimated by simulating how the error in quadrupolar splittings affected the reliability of the tilt angle. Estimates of its value were taken from randomly oriented ^{2}H labeled PLB incorporated in POPC bilayers (Tiburu, E.K. and Lorigan, G.A., unpublished data).

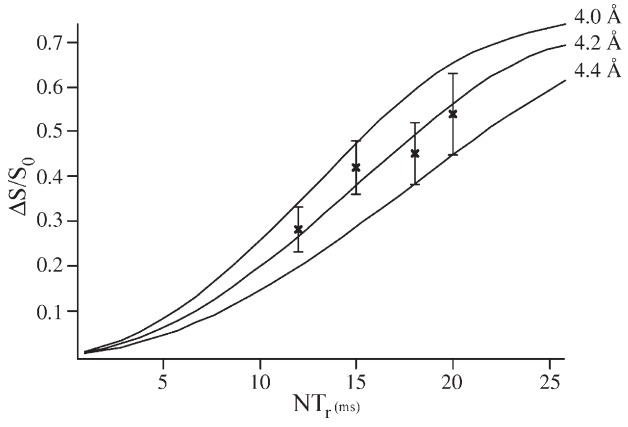

Fig. 3. ^{13}C–^{15}N REDOR data (shown as circles) and simulated REDOR curves to fit the distance measurement. The REDOR simulation curves corresponding to dipolar couplings that yield internuclear distances of 4.0 Å, 4.2 Å, and 4.4 Å are displayed. The best fit is shown in the center with a ^{13}C–^{15}N distance of 4.2 Å.

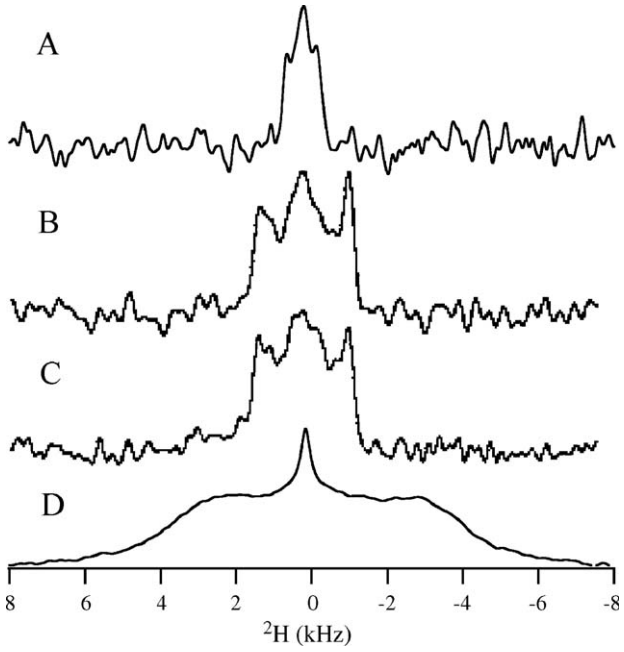

Fig. 4. ^{2}H NMR spectra of ^{2}H-labeled site-specific DOPC/DOPE mechanically aligned phospholipid bilayer samples and randomly oriented control. The spectra were collected at 25 °C. (A) ^{2}H-labeled Leu28, (B) ^{2}H-labeled Leu39, (C) ^{2}H-labeled Leu51, and (D) ^{2}H-labeled Leu28 multi-lamellar vesicle sample for comparison.

4. Discussion

4.1. Secondary structure of TM-PLB in phospholipid bilayers

The appearance of the two peaks in the ^{13}C-CPMAS solid-state NMR experiments shown in Fig. 1A indicates that the TM-PLB peptide is in two different structural conformations in POPC phospholipid bilayers. Previous solid-state NMR

spectroscopic studies have shown two peaks in a similar environment for a ^{13}C-labeled Ala residue for the magainin antimicrobial peptide [29]. In that study, the upfield peak is attributed to either a β-sheet or an unstructured conformation of the peptide. This was confirmed by FTIR and later ^{31}P NMR studies which showed that the β-sheet magainin peptide rests on the outside of the lipid bilayer, while the α-helical portion must have been inserted inside the bilayer [29]. The 3 ppm difference between the two peaks in Fig. 1A is within the 2–6 ppm range exhibited by ^{13}C═O of α-helical proteins and are shifted downfield with respect to those of the β−sheet or unstructured form [66]. The upfield peak is most likely either a random coil or β-sheet structural conformation of the TM-PLB peptide, possibly even aggregated unstructured peptides that did not insert properly into the bilayer. It should be noted that studies of the conformational dependence of the ^{13}C═O chemical shift have been performed in systems that are not in phospholipid bilayers. However, it is not necessary to consider the addition of lipids because the chemical shift of the carbonyl carbons of an α-helical protein are embedded into the center of the α-helix and are shielded from the lipids [67] (Fig. 5).

The addition of a charged phospholipid such as POPG to the POPC phospholipids enhanced the percentage of α-helical TM-PLB components in the membrane protein sample (Fig. 1). This is probably due to the fact that POPG has a net negative charge. The orientation of this charge is such that in molecular dynamic simulations, Na^+ salts surrounding POPC bilayers barely interact with POPC while they interact very frequently with POPG

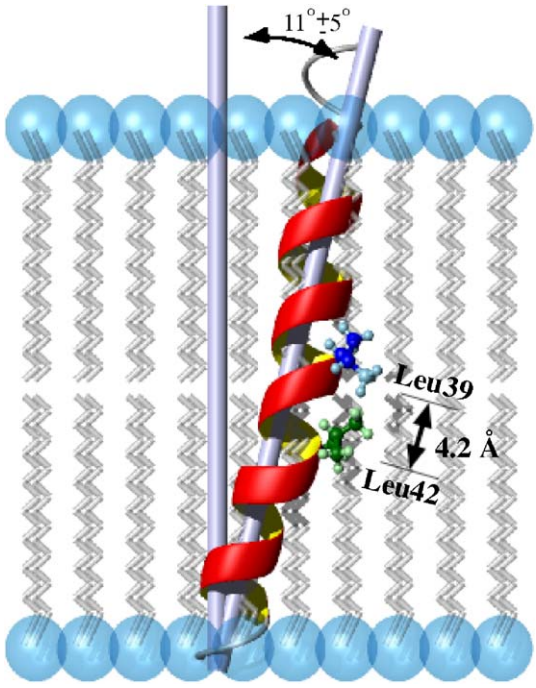

Fig. 5. Model of the transmembrane segment of phospholamban in a phospholipid bilayer. The peptide exists as a pentamer, but is shown as a monomer for clarity. Labels shown are those used in the solid-state NMR experiments and referenced in this paper. The ^{13}C–^{15}N labels measured using the solid-state NMR REDOR technique are shown for clarity.

lipids [68]. After 20 h of sample hydration, the upfield peak attributed to the unstructured/β-sheet conformation of TM-PLB disappeared in the POPC/POPG mixed bilayer. At the same time, the α-helical peak increased dramatically. It would seem that as the phospholipid bilayer is hydrated and forms more completely, the charged POPG phospholipids helps the TM-PLB peptide to fold and insert into the phospholipid bilayer.

Either in addition to helping TM-PLB to properly insert or an alternative explanation of the decreased upfield peak, the addition of the surface charged POPG phospholipids may reduce the formation of unstructured peptide aggregates. It has been reported that upfield peaks of α-carbons in model peptides are caused by the solvation effects and are due only to the structure of the peptide [69]. Recent ab initio calculations and solid-state NMR spectroscopic data have demonstrated that carbonyl carbons are also affected in a similar manner. Thus, it is reasonable to conclude the upfield shifted peak is due to PLB that is in an environment outside the bilayer affected by the water solvent [70, 71]. A likely form of the PLB existing outside the bilayer is as clusters of protein forming aggregates to avoid the hydrophilic water environment. Charges in the bilayer originating from the POPG might cause a breakup of these aggregates or prevent them from forming, resulting in more non-aggregated PLB ready to insert in the bilayers as they are hydrated. The final result is the absence of an unstructured/β-sheet peak and a much more pronounced α-helical peak indicating that the TM-PLB peptide is incorporated more fully into the charged POPC/POPG phospholipid bilayer. Thus, the choice of phospholipid and degree of hydration plays an extremely important role in the structure and folding pattern of the transmembrane segment of PLB. Previous work on this topic has shown that the M1 segment of the nAChR by de Planque et al. also exhibits some conformational dependence on lipid composition and hydration [72].

4.2. REDOR and TM-PLB Structural Model

The hydrophobic thickness of the POPC has been estimated to be about 27 Å [73]. Assuming the number of amino acids per turn in an α-helix is 3.6 residues, and the pitch is 5.4 Å, then the translation per residue along the α-helical peptide will be 1.5 Å. The distance result from the REDOR measurement indicates that there is a translation of 1.4 Å per amino acid along the α-helix. This is very close to a 3.6 amino acid per turn protein. If we take into account the 5 Å polar headgroups of the lipids and the 10° tilt of the protein, it is clear that 27 amino acids can span the POPC bilayer. But, according to Tiburu and coworkers the Leu51 of PLB is located 4 Å below the lipid water interface [16]. This allows space for 25 amino acids to span the bilayer places Leu28 outside the bilayer also in accordance with Tiburu and coworkers [16].

Fig. 4 shows a structural model of TM-PLB in phospholipid bilayers. For clarity, the structure is shown as a monomer. The amino acids and the exact locations where the ^{13}C–^{15}N REDOR distance measurements were taken are highlighted. Several labs have shown that a PLB/lipid mole ratio as low as 1:100 will spontaneously assemble into a pentamer in DOPC phospholipid bilayers [9,74,75]. Since we have used 4 mol% TM-PLB for the

REDOR studies, we expect to have mainly pentameric structural conformations. However, such studies have also indicated the possibility of dynamic exchange between monomeric and pentameric structures of PLB [9,74,75]. It is interesting to note that the α-helix carbonyl carbon peaks in the ^{13}C-REDOR spectra are quite narrow (~250 Hz). Since the frequency of the carbonyl ^{13}C chemical shift is sensitive to secondary structure and hydrogen bonding, the relatively narrow line width indicates that there is not a wide range of conformations in the TM-PLB peptide. Thus, we expect that TM-PLB does not change its torsion angles at Leu37 to go between monomer and pentamer form for we would expect a broader peak if they had different torsional angles [76].

Finally, the 11° tilt of the peptide in the bilayer supports a model of PLB that has its cytosolic portion tilted greater than 50° with respect to the bilayer normal [24]. This is the same as the model proposed for the monomeric TM-PLB that is tilted 10° with respect to the bilayer [19]. Therefore, there is considerable evidence that there is no significant conformation or tilt change of TM-PLB when it goes from its pentamer to its monomeric form. Thus, a conformation change of the transmembrane portion of PLB is most likely not responsible for the mechanism of action of SERCA inhibition. In the transmembrane region near Leu37, the current study agrees with the tilted α-helical nature of the transmembrane region determined in the solution-state NMR study of Chou et al. [18].

5. Conclusion

In conclusion, two important experiments have been described in this paper to investigate the structural properties of pentameric TM-PLB in a variety of different membrane systems through the use of solid-state NMR spectroscopic techniques.

(1) ^{13}C-CPMAS solid-state NMR spectroscopic studies, revealed the folding pattern of TM-PLB in a variety of membranes. The effect of adding a charged POPG phospholipid to a POPC phospholipid bilayer (well and not well hydrated) significantly increased the number of α-helical structural components of TM-PLB in the membrane. In addition, the α-helical structure of the protein was further supported by the unique chemical shift of the ^{13}C CPMAS spectra. (2) Solid-state NMR ^{13}C–^{15}N REDOR data were used to measure distance constraints over two different residues on the TM-PLB peptide in POPC/POPG lipid bilayers. The ^{13}C–^{15}N distance between the leucine residues of 42 and 39 was determined to be 4.2 Å and agrees well with the α-helical structure of TM-PLB. (3) The tilt angle of PLB with respect to the lipid bilayer normal of 11°±5° and the sharp peak width of the ^{13}C CPMAS spectrum of α-helical PLB indicate limited differences between the monomeric and pentameric transmembrane sections of PLB.

Acknowledgements

This work was supported by the American Heart Association Scientist Development Grant (#0130396N) and a NIH Grant (GM60259-01). The 500 MHz Wide bore NMR Spectrometer was obtained from NSF Grant (#10116333). ESK would like to thank the Arnold O. Beckman for financial support. We acknowledge help from Mr. Krishnan Damodaran with the NMR experiments.

References

[1] S.J. Opella, NMR and membrane proteins, Nat. Struct. Biol. 4 (1997) 845–848.
[2] S.J. Opella, A. Nevzorov, M.F. Mesleh, F.M. Marassi, Structure determination of membrane proteins by NMR spectroscopy, Biochem. Cell Biol. Biochim. Biol. Cell. 80 (2002) 597–604.
[3] T.A. Cross, S.J. Opella, Solid-state NMR structural studies of peptides and proteins in membranes, Curr. Opin. Struck. Biol. 4 (1994) 574–581.
[4] F.M. Marassi, S.J. Opella, NMR structural studies of membrane proteins, Curr. Opin. Struck. Biol. 8 (1998) 640–648.
[5] L.K. Thompson, Solid-state NMR studies of the structure and mechanisms of proteins, Curr. Opin. Struck. Biol. 12 (2002) 661–669.
[6] D.E. Warschawski, M. Traikia, P.F. Devaux, G. Bodenhausen, Solid-state NMR for the study of membrane systems: the use of anisotropic interactions, Biochimie 80 (1998) 437–450.
[7] H. Li, M.J. Cocco, T.A. Steitz, D.M. Engelman, Conversion of phospholamban into a soluble pentameric helical bundle, Biochemistry 40 (2001) 6636–6645.
[8] D.H. MacLennan, E.G. Kranias, Phospholamban: a crucial regulator of cardiac contractility, Nature 4 (2003) 566–578.
[9] R.L. Cornea, L.R. Jones, J.M. Autry, D.D. Thomas, Mutation and phosphorylation change the oligomeric structure of phospholamban in lipid bilayers, Biochemistry 36 (1997) 2960–2967.
[10] H.K. Simmerman, Y.M. Kobayashi, J.M. Autry, L.R. Jones, A leucine zipper stabilizes the pentameric membrane domain of phospholamban and forms a coiled-coil pore structure, J. Biol. Chem. 271 (1996) 5941–5946.
[11] E. Hughes, D.A. Middleton, Solid-state NMR reveals structural changes in phospholamban accompanying the functional regulation of Ca^{2+}-ATPase, J. Biol. Chem. 278 (2003) 20835–20842.
[12] J.P. Schmitt, M. Kamisago, M. Asahi, J.L. Guo, F. Ahmad, U. Mende, E.G. Kranias, D.H. MacLennan, J.G. Seidman, C.E. Seidman, Dilated cardiomyopathy and heart failure caused by mutation in phospholamban, Science 299 (2003) 1410–1413.
[13] A. Mascioni, C. Karim, J. Zamoon, D.D. Thomas, G. Veglia, Solid-state NMR and rigid body molecular dynamics to determine domain orientations of monomeric phospholamban, J. Am. Chem. Soc. 124 (2002) 9392–9393.
[14] S. Lamberth, H. Schimidt, M. Muenchbach, T. Vorherr, J. Krebs, E. Carafoli, C. Griesinger, NMR solution structure of phospholamban, Helv. Chim. Acta 83 (2000) 2141–2152.
[15] P. Pollesello, A. Annila, M. Ovaska, Structure of the 1–36 amino-terminal fragment of human phospholamban by nuclear magnetic resonance and modeling of the phospholamban pentamer, Biophys. J. (1999) 1784–1795.
[16] E.K. Tiburu, E.S. Karp, P.C. Dave, K. Damodaran, G.A. Lorigan, Investigating the dynamic properties of the transmembrane segment of phospholamban incorporated into phospholipid Bilayers utilizing 2H and 15N solid-state NMR spectroscopy, Biochemistry 43 (2004) 13899–13909.
[17] Z. Ahmed, D.G. Reid, A. Watts, D.A. Middleton, A solid-state NMR study of the phospholamban transmembrane domain: local structure and interactions with Ca2+-ATPase, Biochim. Biophys. Acta 1468 (2000) 187–198.
[18] K. Oxenoid, J. Chou, The structure of phospholamban pentamer reveals a channel-like architecture in membranes, PNAS 102 (2005) 10870–10875.
[19] I.T. Arkin, M. Rothman, C.F. Ludlam, S. Aimoto, D.M. Engelman, K.J. Rothschild, S.O. Smith, Structural model of the phospholamban ion channel complex in phospholipid membranes, J. Mol. Biol. 248 (1995) 824–834.
[20] S.A. Tatulian, L.R. Jones, L.G. Reddy, D.L. Stokes, L.K. Tamm, Secondary structure and orientation of phospholamban reconstituted in supported bilayers from polarized attenuated total reflection FTIR spectroscopy, Biochemistry 34 (1995) 4448–4456.
[21] I.T. Arkin, P.D. Adams, A.T. Brunger, S. Aimoto, D.M. Engelman, S.O. Smith, Structure of the transmembrane cysteine residues in phospholamban, J. Membr. Biol. 155 (1997) 199–206.

[22] J. Zamoon, A. Mascioni, D.D. Thomas, G. Veglia, NMR solution structure and topological orientation of monomeric phospholamban in dodecylphosphocholine micelles, Biophys. J. 85 (2003) 2589–2598.
[23] D.A. Middleton, Z. Ahmed, C. Glaubitz, A. Watts, REDOR NMR on a hydrophobic peptide in oriented membranes, J. Magn. Reson. 147 (2000) 366–370.
[24] S.O. Smith, T. Kawakami, W. Liu, M. Ziliox, S. Aimoto, Helical structure of phospholamban in membrane bilayers, J. Mol. Biol. 313 (2001) 1139–1148.
[25] A.C. de Dios, J.G. Pearson, E. Oldfield, Secondary and tertiary structural effects on protein NMR chemical shifts: an ab initio approach, Science 260 (1993) 1491–1496.
[26] G.R. Marshall, D.D. Beusen, K. Kociolek, A.S. Redlinski, M.T. Leplawy, Y. Pan, J. Schaefer, Determination of a precise interatomic distance in a helical peptide by REDOR NMR, J. Am. Chem. Soc. 112 (1990) 963–966.
[27] J. Yang, D.P. Weliky, Solid-state nuclear magnetic resonance evidence for parallel and antiparallel strand arrangements in the membrane-associated HIV-1 fusion peptide, Biochemistry 42 (2003) 11879–11890.
[28] J. Yang, P.D. Parkanzky, M.L. Bodner, C.A. Duskin, D.P. Weliky, Application of REDOR subtraction for filtered MAS observation of labeled backbone carbons of membrane-bound fusion peptides, J. Magn. Reson. 159 (2002) 101–110.
[29] D.J. Hirsh, J. Hammer, W.L. Maloy, J. Blazyk, J. Schaefer, Secondary structure and location of a magainin analog in synthetic phospholipid bilayers, Biochemistry 35 (1996) 12733–12741.
[30] H. Saito, Conformation-dependent carbon-13 chemical shifts: a new means of conformational characterization as obtained by high-resolution solid-state carbon-13 NMR, Magn. Reson. Chem. 24 (1986) 835–852.
[31] E. Oldfield, Chemical shifts and three-dimensional protein structures, J. Biol. NMR 5 (1995) 217–225.
[32] D.S. Wishart, B.D. Sykes, The 13C chemical-shift index: a simple method for the identification of protein secondary structure using 13C chemical-shift data, J. Biomol. NMR 4 (1994) 171–180.
[33] D.S. Wishart, B.D. Sykes, F.M. Richards, Relationship between nuclear magnetic resonance chemical shift and protein secondary structure, J. Mol. Biol. 222 (1991) 311–333.
[34] A.C. de Dios, E. Oldfield, Recent progress in understanding chemical shifts, Solid State NMR 6 (1996) 101–125.
[35] I. Ando, T. Kameda, N. Asakawa, S. Kuroki, H. Kurosu, Structure of peptides and polypeptides in the solid state as elucidated by NMR chemical shift, J. Mol. Struct. 441 (1998) 213–230.
[36] E.K. Tiburu, P.C. Dave, J.F. Vanlerberghe, T.B. Cardon, R.E. Minto, G.A. Lorigan, An improved synthetic and purification procedure for the hydrophobic segment of the transmembrane peptide phospholamban, Anal. Biochem. 318 (2003) 146–151.
[37] A. Naito, K. Nishimura, S. Kimura, S. Tuzi, M. Aida, N. Yasuoka, H. Saito, Determination of the three-dimensional structure of a new crystalline form of N-Acetyl-Pro-Gly-Phe as revealed by 13C REDOR, X-Ray diffraction, and molecular dynamics calculation, J. Phys. Chem. 100 (1996) 14995–15004.
[38] A. Pines, M.G. Gibby, W. JS, Proton enhanced NMR of dilute spins in solids, J. Chem. Phys. 59 (1973) 569–590.
[39] J.H. Davis, K.R. Jeffrey, M. Bloom, M.I. Valic, Quadrupolar echo deuterium magnetic resonance spectroscopy in ordered hydrocarben chains, Chem. Phys. Lett. 42 (1976) 390–394.
[40] T. Gullion, D.B. Baker, M.S. Conradi, New, compensated Carr–Purcell sequences, J. Magn. Reson. 89 (1990) 479–484.
[41] E. Strandberg, S. Ozdirekcan, D.T.S. Rijkers, P.C.A. van der Wel, R.E. Koeppe II, R.M.J. Liskamp, J.A. Killian, Tilt angles of transmembrane model peptides in oriented and non-oriented bilayers as determined by 2H solid-state NMR, Biophys. J. 86 (2004) 3709–3721.
[42] J.A. Whiles, K.J. Glover, R.R. Volde, E.A. Komives, Methods for studying transmembrane peptides in bicelles: consequences of hydrophobic mismatch and peptide sequence, J. Magn. Reson. 158 (2002) 149–156.
[43] J.A. Whiles, R. Brasseur, K.J. Glover, R.R. Vold, G. Malacini, E.A. Komives, Orientation and effects of mastoparan X on phospholipid bicelles, Biophys. J. 80 (2001) 280–293.
[44] D.H. Jones, K.R. Barber, E.W. VanDerLoo, W.M. Grant, Epidermal factor receptor transmembrane domain: 2H NMR implications for orientation and motion in a bilayer environment, Biochemistry 37 (1998) 16780–16787.
[45] S. Lamberth, H. Schmidt, M. Muenchbach, T. Vorherr, J. Krebs, E. Carafoli, C. Griesinger, NMR solution structure of phospholamban, Helv. Chim. Acta 83 (2000) 2141–2152.
[46] H. Lee, S. Huo, T.A. Cross, Lipid–peptide interface: valine conformation and dynamics in the gramicidin channel in a lipid bilayer, Biochemistry 34 (1995) 857–867.
[47] H.C. Lee, T.A. Cross, Side-chain structure and dynamics at the lipid–protein interface: ValI of the gramicidin A channel, Biophys. J. 66 (1994) 1380–1387.
[48] T. Gullion, J. Schaefer, Rotational-echo double-resonance NMR, J. Magn. Reson. 81 (1989) 196–200.
[49] T. Gullion, Elimination of resonance offset effects in rotational-echo double-resonance NMR, J. Magn. Reson. 92 (1991) 439–442.
[50] V. Bork, T. Gullion, A. Hing, J. Schaefer, Measurement of 13C-15N coupling by dipolar-rotational spin-echo NMR, J. Magn. Reson. 88 (1990) 523–532.
[51] T. Gullion, Introduction to rotational-echo double-resonance spectroscopy, Concepts Magn. Reson. 10 (1998) 277–289.
[52] Y. Pan, T. Gullion, J. Schaefer, Determination of C–N internuclear distances by rotational-echo double-resonance NMR of solids, J. Magn. Reson. 90 (1990) 330–340.
[53] A. Naito, K. Nishimura, S. Kimura, S. Tuzi, M. Aida, N. Yasuoka, H. Saito, Determination of the three-dimensional structure of a new crystalline form of N-acetyl-pro-gly-phe as revealed by 13C REDOR, X-ray diffraction, and molecular dynamics calculations, J. Phys. Chem. 100 (1996) 14995–15004.
[54] J.R. Garbow, C.A. Mcwherter, Determination of the molecular conformation of melanostatin using 13C, 15N-REDOR NMR spectroscopy, J. Am. Chem. Soc. 115 (1993) 238–244.
[55] P.C. Dave, E.K. Tiburu, K. Damodaran, G.A. Lorigan, 31P and 2H Solid-State NMR Spectroscopic Studies of the Transmembrane Domain of the Membrane-Bound Protein Phospholamban, Biophys. J. 86 (2004) 1564–1573.
[56] T. Gullion, J. Schaefer, Rotational-echo double-resonance NMR, J. Magn. Reson. (1969–1992) 81 (1989) 196–200.
[57] T. Gullion, J. Schaefer, Elimination of resonance offset effects in rotational-echo, double-resonance NMR, J. Magn. Reson. 92 (1991) 439–442.
[58] V. Bork, T. Gullion, A. Hing, J. Schaefer, Measurement of carbon-13–nitrogen-15 coupling by dipolar-rotational spin-echo NMR, J. Magn. Reson. 88 (1990) 523–532.
[59] A. Naito, T. Nagao, K. Norisada, T. Mizuno, S. Tuzi, H. Saito, Conformation and dynamics of melittin bound to magnetically oriented lipid bilayers by solid-state 31P and 13C NMR Spectroscopy, Biophys. J. 78 (2000) 2405–2417.
[60] R. Smit, F. Separovic, T.J. Milne, A. Whittaker, F.M. Bennett, B.A. Cornell, A. Makriyannis, Structure and orientation of the pore-forming peptide, melittin, in lipid bilayers, J. Mol. Biol. 241 (1994) 456–466.
[61] B.A. Cornell, F. Separovic, R. Smith, A.J. Baldassi, Conformation and orientation of gramicidin A in oriented phospholipid bilayers measured by solid state carbon-13 NMR, Biophys. J. 53 (1988) 67–76.
[62] E. Lindahl, O. Edholm, Dynamics simulation of NMR relaxation rates and slow dynamics in lipid bilayers, J. Chem. Phys. 114 (2001) 4938–4950.
[63] J. Yang, P.D. Parkanzky, M.L. Bodner, C.A. Duskin, D.P. Weliky, Application of REDOR subtractions for filtered MAS observation of labeled backbone carbons of membrane-bound fusion peptides, J. Magn. Reson. 159 (2002) 101–110.
[64] M.R.R. de Planque, E. Goormaghtigh, D.V. Greathouse, R.E. Koeppe II, J.A.W. Kruijtzer, R.M.J. Liskamp, B. de Kruijff, J.A. Killian, Sensitivity of single membrane-spanning a-helical peptides to hydrophobic mismatch with a lipid bilayer: Effects on backbone structure, orientation, and extent of membrane incorporation, Biochemistry 40 (2001) 5000–5010.
[65] K.P. Howard, S.J. Opella, High-resolution solid-state NMR spectra of integral membrane proteins reconstituted into magnetically oriented phospholipid bilayers, J. Magn. Reson. B 112 (1996) 91–94.
[66] H. Saito, S. Tuzi, S. Yamaguchi, S. Kimura, M. Tanio, M. Kamihira, K. Nishimura, A. Naito, Conformation and dynamics of membrane proteins and biologically active peptides as studied by high-resolution solid-state 13C NMR, J. Mol. Struct. 441 (1998) 137–148.

[67] S. Kimura, A. Naito, S. Tuzi, H. Saito, A 13C NMR study on [3–13C]-, [1–13C]Ala-, or [1–13C]Val-labeled transmembrane peptides of bacteriorhodopsin in lipid bilayers: insertion, rigid-body motions, and local conformational fluctuations at ambient temperature, Biopolymers 58 (2001) 78–88.
[68] T. Rog, K. Murzyn, M. Pasenkiewicz-gierula, Molecular dynamics simulations of charged and neutral lipid bilayers: Treatment of electrostatic interactions, Acta Biochim. Pol. 50 (2003) 789–798.
[69] D.S. Wishart, B.D. Sykes, F.M. Richards, Relationship between nuclear magnetic resonance chemical shift and protein secondary structure, J. Mol. Biol. 222 (1991) 311–333.
[70] Y. Wei, D.K. Lee, A. Ramamoorthy, Solid-state 13C NMR chemical shift anisotropy tensors of polypeptides, J. Am. Chem. Soc. 123 (2001) 6118–6126.
[71] J. Birn, A. Poon, Y. Mao, A. Ramamoorthy, Ab initio study of 13C-alpha chemical shift anisotropy tensors in peptides, J. Am. Chem. Soc. 126 (2004) 8529–8534.
[72] M.R.R. de Planque, D.T.S. Rijkers, J. Fletcher, R.M.J. Liskamp, F. Separovic, The alpha-M1 segment of the nicotinic acetylcholine receptor exhibits conformational flexibility in a membrane environment, Biochim. Biophys. Acta 1665 (2004) 40–47.
[73] B.A. Cornell, F. Separovic, Membrane thickness and acyl chain length, Biochim. Biophys. Acta 733 (1983) 189–193.
[74] M. Li, L.G. Reddy, R. Bennett, N.D. Silva, L.R. Jones, D.D. Thomas, A fluorescence energy transfer method for analyzing protein oligomeric structure: application to phospholamban, Biophys. J. 76 (1999) 2587–2599.
[75] L.G. Reddy, L.R. Jones, D.D. Thomas, Depolymerization of phospholamban in the presence of calcium pump: a fluorescence energy transfer study, Biochemistry 38 (1999) 3954–3962.
[76] J. Colyer, Phosphorylation states of phospholamban, Ann. N. Y. Acad. Sci. 853 (1998) 79–91.